European Polymer Journal 121 (2019) 109292

Contents lists available at ScienceDirect

European Polymer Journal

journal homepage: www.elsevier.com/locate/europolj

New ultrastiff bio-furan epoxy networks with high T_g: Facile synthesis to excellent properties

Jingjing Meng[a], Yushun Zeng[a], Pengfei Chen[a], Jie Zhang[a], Cheng Yao[b], Zheng Fang[a], Kai Guo[a]

[a] College of Biotechnology and Pharmaceutical Engineering, Nanjing Tech University, Nanjing 211816, PR China
[b] College of Chemistry and Molecular Engineering, Nanjing Tech University, Nanjing 211816, PR China

ARTICLE INFO

Keywords:
Stiffness
Biomass
Epoxy resin
Flame retardancy
Thermomechanical properties
Mechanical properties

ABSTRACT

Novel resins were synthesized from diglycidyl ester of 2,5-furandicarboxylic acid (DGF) and 3,3′-diamino diphenylsulfone (33DDS) and 4,4′-diamino diphenyl-sulfone (44DDS), respectively. The networks possessed ultra high stiffness (E'= 4.02 GPa) and the highest T_g (216 °C) in biomass-based epoxy resins to date, which allows their potential applications in many cutting-edge areas.

1. Introduction

With the development of extraction and refining technology, petrochemical intermediates greatly upgrade our living standards. Various traditional polymers, such as polyesters, polyurethane, polyamides and epoxy resins are commonly manufactured. For instance, epoxy resins have been widely explored and consumed. They play a significant role in the fields, such as electronics, motor vehicles, auto parts & accessories as well as household decorations, and so on [1]. To our knowledge, approximately 90% of epoxy networks are manufactured from the fossil-based bisphenol A (BPA) [2]. The disposable nature of thermosets drove the demands of nonrenewable resources, especially for petroleum-based bisphenol A. It was reported that the annual global production of epoxy had reached more than 3 million tons from 2017 [3]. Despite a sharp production in the past decades, it cannot be denied that the growing depletion has led to the poverty of fossil resources.

However, several restraints such as fluctuating raw material prices, the threat from alternatives, and low bio-safety issues have lessened the diglycidyl ether of bisphenol A (DGEBA) market structures. In particular, the issues on the carcinogenicity, mutagenicity, reprotoxicity, endocrine disruptors and reproductive health effects induced by BPA, have given rise to the public attention [4]. Recently, great attempts have been devoted to biomass-derivated epoxy resins instead of the petrochemical stocks [2,5]. Numerous biomass alternatives, for instance, vannilin [6,7], eugenol [8,9], daidzein [3], itaconic acid [10], are disclosed with superior performances. Other than those renewable resources, polymeric networks from sugar derivatives, *e.g.*, isosorbide [11,12], 2,5-furandicarboxylic acid (FDCA) [13,14] and 5-(hydroxymethyl) furfural (5-HMF) [15–18], etc. emerged. Recent years have witnessed a rapid growth in biobased epoxy resins, which were expected to substitute the petro-based analogs [19]. Of those sugar-based biomasses, FDCA had been deemed as a top ten green chemical by the U.S. Department of Energy (DOE) in 2004 [15]. The continuous availability and the environmental sustainability of the FDCA determined that it is a reasonable alternative to the BPA fossil stock.

However, in the past decades, few concerns about FDCA's applications in thermosets were sparked. In 2015, Liu et al. first synthesized 2,5-furandicarboxylic acid (DGF) via a facile reaction between FDCA and epichlorohydrin. It was then cured by methylhexahydrophthalic anhydride (MHHPA) and poly(propylene glycol) bis(2-aminopropyl ether) (D230), respectively. Notably, the resultant DGF/MHHPA networks behaved higher curing reactivity and elevated glass transition temperature (T_g = 152 °C) [13]. In 2018, Johansson reported the DGF/epoxidized fatty methyl esters thermosets with full biomass blocks via cationic polymerization. The fatty acids significantly enhanced the reaction rate when UV-curing occurred [14]. Unexpectedly, no more than two pieces of literature had been reported about the DGF-based epoxy resins. Moreover, for the renewable epoxy matrixes, there yet remain several disadvantages, such as (1) The sugar-based epoxy resins with T_g more than 200 °C are hardly developed, other than the N/P-enhanced eugenol [20–22] and the newly daidzein epoxy resins [3] (Scheme 1). (2) Sustainable networks with excellent stiffness in a wide temperature range are scarcely revealed. Up to now, a solitary instance, *i.e.* TEU-EP/33DDS network (1 GPa ~3.7 GPa, 25–190 °C, Table S2, ESI), was reported by Wang [22]. (3) Solvent-free polymerization of crystalline DGF building blocks was never established [13]. Overall, reliable

E-mail address: guok@njtech.edu.cn (K. Guo).

https://doi.org/10.1016/j.eurpolymj.2019.109292
Received 16 August 2019; Received in revised form 29 September 2019; Accepted 4 October 2019
Available online 08 October 2019
0014-3057/ © 2019 Elsevier Ltd. All rights reserved.

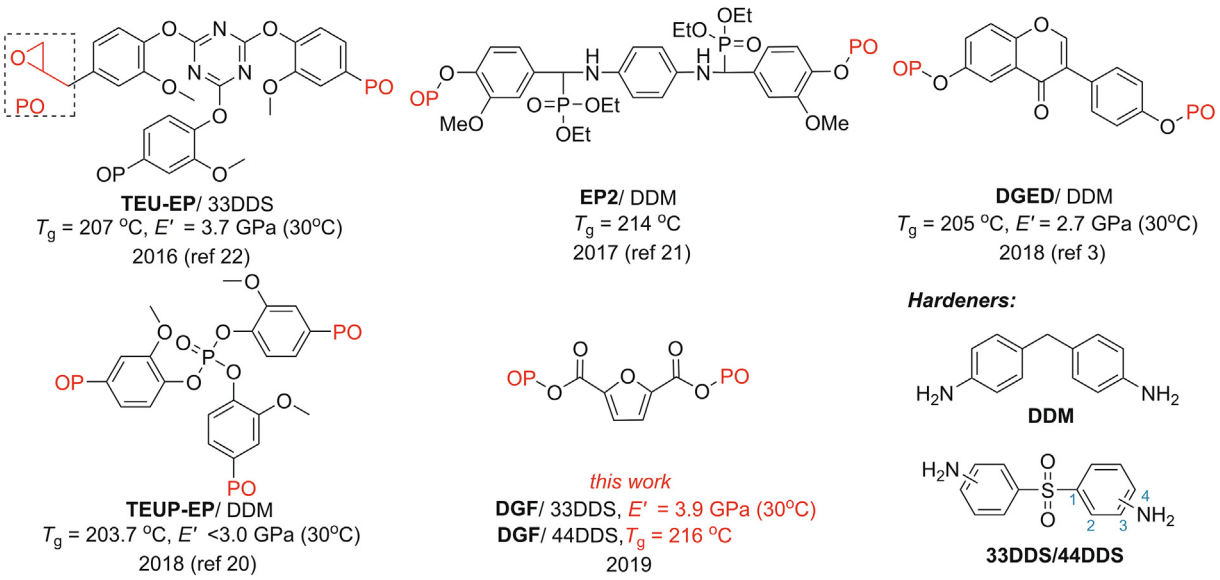

Scheme 1. Biomass-based epoxy resin with high T_gs and excellent storage moduli.

approaches for the biomass-based epoxy networks overcoming such shortcomings met with great challenges.

Herein, based on FDCA, DGF monomer was efficiently produced and used for polymeric networks via a solvent-free approach, and the related mechanical and thermal properties are intensively investigated. In comparison with the petrochemical DGEBA/DDS networks, the sugar-based DGF/DDS composites behaved with super stiffness and displayed the highest T_g among biomass-based epoxy resins. This work ensures us a new strategy for the preparation of preferable performance epoxy resins with a wide operating temperature range.

2. Results and discussion

Initially, commercial FDCA was employed to yield DGF monomer. As shown in Scheme 2. FDCA was blended with allyl bromide under the mild condition for about 2 days, and readily yielded intermediate 2,5-bis((allyloxy)methyl)furan (BAMF) in 85%. The successive oxidation catalyzed by *m*-CPBA afforded the DGF monomer in 75%. When FDCA was used as starting material, the purifying processes via a continuous distillation/recrystallization made it critical for safely performing the scale-up reactions, thus ensuring a much more feasible protocol for sustainable technologies. Subsequently, with DGF and commonly prevalent DGEBA in hands, the curing processes were conducted, wherein 3, 3′-diamino diphenyl-sulfone (33DDS) and 4, 4′-diamino diphenyl-sulfone (44DDS) were employed as hardeners yielding DGF/DDS and DGEBA/DDS networks. The curing procedure occurred via a solvent-free protocol, where the stoichiometric ratios for DGEBA/DDS and DGF/DDS are 100/36.4 and 100/46.2 (w/w), respectively. The blends of epoxide and DDS were degasified under argon and vigorously stirred for 30 min. The homogeneously molten mixture (120–160 °C) with lower viscosities was injected into a preheated molding (80 °C), and then moved into curing reactor ranging from 185 °C to 235 °C in pure argon flow. The curing reactor climbed up to the specific curing temperature in 1 h and then maintained for additional 2 h. After being cooling naturally, the ejection of the casting from the molds proceeded.

The IR technique was used to determine the variation of characteristic peaks of NH_2 and oxirane in the curing process. As Fig. 1 has shown, for 44DDS hardener, the characteristic absorptions of NH_2 groups lied in 1625 cm^{-1} (NH_2, bending vibration), 3327 and 3357 cm^{-1} (stretching vibration). Analogously, the absorption peaks at 1623, 3352 and 3382 cm^{-1} correspond to the 33DDS. In addition, the characteristic bands of aromatic rings are composed of 1400–1600 cm^{-1} (aromatic C=C stretching) and 650–900 cm^{-1} (C–H deformation). Other than the typical peaks of the aromatic ring, the peaks appear at 858, 907 and 1239 cm^{-1} were attributed to oxiranes for DGEBA. In terms of DGF, identical oxirane peaks exist at 860, 909, 1239 cm^{-1}. The peak at 1745 cm^{-1} indicates the carbonyl stretching, while 1030, 1184, 1510 cm^{-1} represent the furan rings [15]. For the fully cured networks, curves for DGF/DDS disclosed that the typical peaks of oxirane (860 and 909 cm^{-1}) and NH_2 (about 1623 cm^{-1}) disappeared. Such variations happened to DGEBA/DDS networks as well. Therefore, it was demonstrated that the oxiranes/DDS systems were fully cured and the DGF/DDS polymers were furnished.

The thermal curing behaviors of DGF/DDS and DGEBA/DDS systems were explored by differential scanning calorimetry (DSC). The second heating DSC curves of those networks are shown in Fig. 2a and b. The lower curing temperatures for DGF comparable to that of DGEBA suggested that the DGF was more active than DGEBA (Table S1, ESI). The increased reactivity could be attributed to the higher polarizability of the epoxy rings in DGF [13]. The ester function is more polar than the ether, which significantly withdraws electron from the neighboring epoxy ring and enhances the reactivity. Thus an efficient ring opening

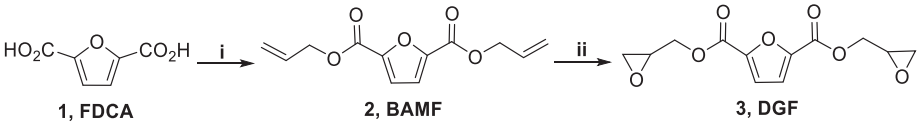

[a] Reaction conditions: (i) FDCA (21.2 g, 1.0 equiv.), K_2CO_3 (56.2 g, 3.0 equiv.), allyl bromide (49.2 g, 3.0 equiv.) in DMF (80 mL), 2 days, rt. 85% yield; (ii) BAMF (11.8 g, 1.0 equiv.), chloroperoxybenzoic acid (21.5 g, 2.5 equiv.), CH_2Cl_2 (50 mL), for 40 °C, 3 days, 75% yield.

Scheme 2. Synthesis of the diglycidyl ester of 2,5-furandicarboxylic acid (DGF)[a].

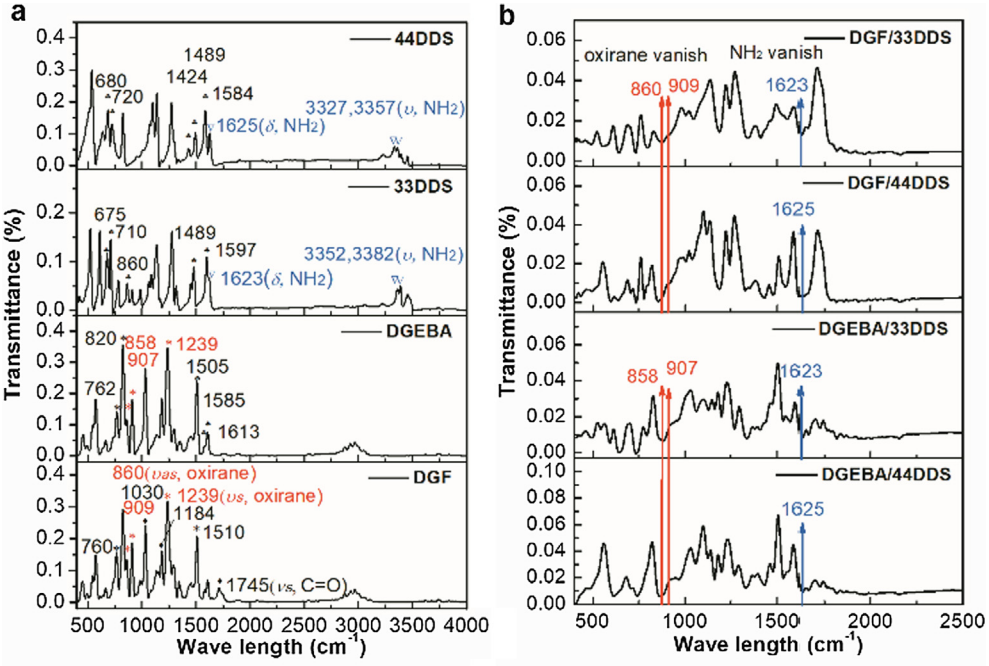

Fig. 1. IR spectra for (a) monomers and (b) polymeric networks.

reaction of DGF monomer readily furnished bio-based epoxy resins at relatively low temperature [23]. Specifically, when symmetric 44DDS was employed, the curing temperature of DGF/44DDS was 50 °C less than for DGEBA/44DDS.

It was reported that asymmetric 33DDS displayed higher reactivity than 44DDS, which dominated the crosslinking processes thereby leading to a higher density [24]. Although the relatively disordered fracture morphology appeared for DGF/33DDS, multiple hydrogen bonds in the networks significantly enhanced the thermomechanical properties [25]. As the SEM images (Fig. 2c and d) shown, it was clearly demonstrated that DGF/33DDS polymers presented densely irregular arrays in contrast to the rod-like tissues in order for DGF/44DDS. The regular polymer packing in the polymers favored an increasing high crystallinity [26]. Therefore, the 33DDS networks possessed relatively low T_g values (Fig. 2a and b). It is worth noting that the DGF/44DDS formulation exhibits a high T_g value. To the best of our knowledge, There is no doubt that DGF/44DDS owns the highest T_g value among the biobased epoxy resins (Table S2, ESI) [3,18,20–22]. As a result, the superiority of DGF/DDS networks significantly guaranteed their long-term performances in thermosetting resins.

Fig. 3 reveals degradation curves for all epoxy networks cured by DDS. To estimate the thermal stabilities of those thermosets, the typical parameters, such as T_{d5} (for 5% degradation), T_{d30} (for 30% degradation) and T_{max} (for the maximum decomposition rates) as well as R_{800} (char residue at 800 °C), are listed in Table 1. Obviously, the DGF/DDS networks present relatively lower initial decomposition temperatures (T_{d5}) in contrast to its DGEBA counterparts (entries 3, 4 *vs.* 1, 2, Table 1). The differential thermogravimetry (DTG) curves suggest that two decomposition stages have happened to DGF/DDS polymers ranging from 300 °C to 500 °C (Fig. 3). Moreover, the DGF/DDS networks started to degrade at about 324 °C above the T_gs, thus indicating their wide working temperature range. It is speculated that DGF motifs are responsible for the first decomposition stage (about 340 °C) of biopolymers, while the dissociation of DDS accounts for the second ones (about 400 °C). From the DTG profiles (Fig. 3b), it is noticed that the DGEBA/DDS decomposes faster than the DGF polymers. Because a large amount of the overflowing carbon occurred in the dramatic exothermic combustion, the DGEBA/DDS polymers yielded less residual chars (entries 3 and 4, Table 1). The highly inflammable DGEBA possibly preferred a sustained burning. Besides, compared to 33DDS, the oxirane cured by 44DDS possessed a relatively low carbon residue. Since a more rapid exothermic process helps to promote decomposition, the sharp decomposition of 44DDS possibly accounts for the slight difference (entries 1 *vs.* 2, 3 *vs.* 4, Table 1; Figure S1-b, ESI). The dynamic thermomechanical analysis (DMA) curves are shown in Fig. 4. In terms of thermomechanical properties, such as glass transition temperature and storage modulus, the DGF/DDS system outperformed its DGEBA/33DDS counterpart in the entire experimental temperature. In the glassy plateau temperature region, for instance, the respective storage moduli (E') at 150 °C for DGF/33DDS, DGF/44DDS, DGEBA/33DDS,

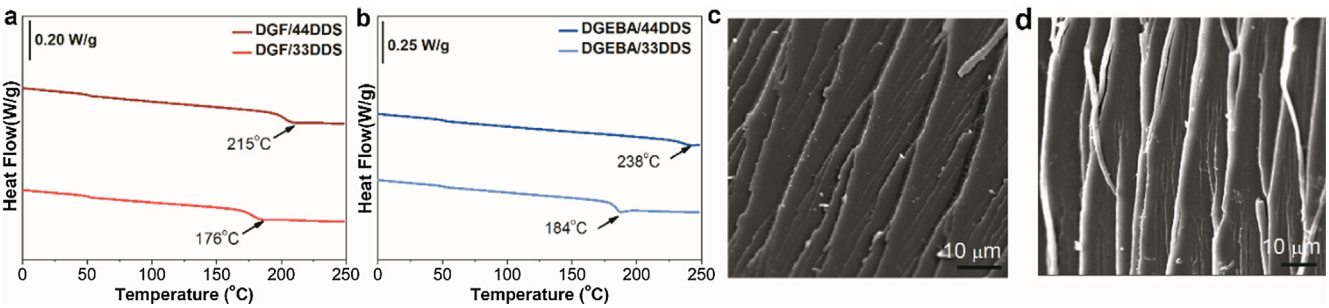

Fig. 2. DSC curves of (a) DGF/DDS and (b) DGEBA/DDS; the morphology of fracture surfaces of (c) DGF/33DDS and (d) DGF/44DDS networks.

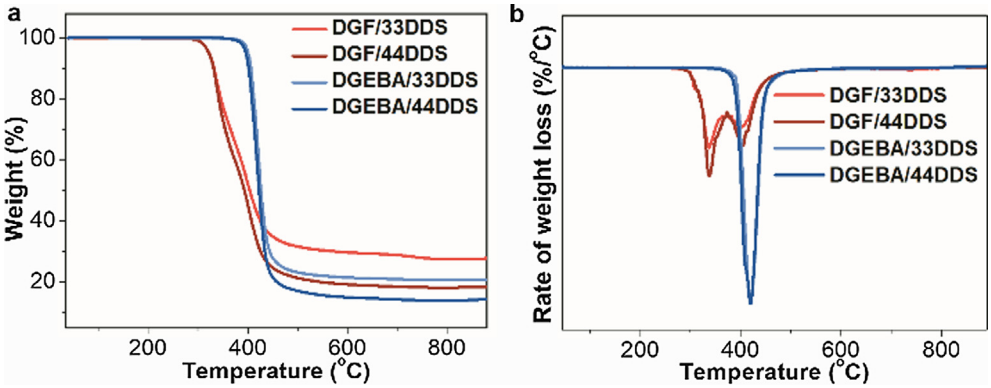

Fig. 3. The degradation curves for DGF/DDS and DGEBA/DDS.

Table 1
Thermal properties in DSC and TGA experiments.

Entry	Sample	T_g[a] (°C)	T_{d5} (°C)	T_{d30} (°C)	T_{max}[b] (°C)	R_{800} (%)
1	DGF/33DDS	176	324	366	337/396	27
2	DGF/44DDS	215	324	355	339/405	18
3	DGEBA/33DDS	184	405	417	418	20
4	DGEBA/44DDS	238	397	414	420	14

[a] From the DSC curves.
[b] The maximum temperature of DTG peaks.

DGEBA/44DDS are 3.09 GPa, 1.76 GPa, 1.21 GPa and 1.12 GPa, respectively. It indicates that the novel DGF/DDS polymers are suitable for high- temperature operations, even being applied to many top-end fields with its unique high stiffness [27]. To the best of our knowledge, up to now, there exists no biobased epoxy resin could reach such a high storage modulus ranging from 0 °C to 180 °C [28].

It is well known that the glass transition temperature (T_g) is a crucial parameter that decides the application filed for thermosets. In Fig. 4b, the cured DGF/33DDS and DGF/44DDS respectively displayed T_g of 180 °C, 216 °C, which were in close accordance with the DSC results. The peak widths at half-height of tan δ for DGF/DDS are wider than for DGEBA/DDS, indicating a broader range of cooperative segment motions involved in the relaxation of DGF systems [29]. Note here that a large amount of H-bond interaction in the DGF/DDS arrays restricted the segmental movement [17,25]. Therefore, the elevated E' and the highest T_g further proved that the FDCA-derived epoxy resins behaved excellent thermomechanical properties. Interestingly, in Fig. 4b, the glass transition peak for the DGEBA/33DDS network had a low-temperature shoulder while DGEBA was employed. It possibly resulted from the phenyl ring flips forced longer range cooperative motions during the heating process of DMA determination [30].

Aside from the H-bond, a higher density occurred due to a greater chain packing, which was beneficial to a higher E' values [31]. The polymers with high E' tended to behave great stiffness and serve as attractive alternatives to DGEBA composites. To elaborate the difference, the crosslink density (v_e) is obtained for rubbery elasticity, wherein E' denotes the storage modulus in the rubbery plateau region at ($T_{g,\ DMA}$ + 30) °C, T ($T_{g,\ DMA}$ + 30) (K) signifies the absolute temperature, and R refers to the gas constant.

$$v_e = E'/(3RT)$$

The results are listed in Table 2. Apparently, the DGF/33DDS exhibited a significantly high crosslink density. Comparably, DGF/44DDS was less crosslinked (entry 1 *vs.* 2, Table 2). Moreover, it is noted that the slight difference in v_e values does not discriminate DGEBA/33DDS from DGEBA/44DDS. However, in contrast to DGEBA/33DDS, DGF/44DDS with relatively low density possessed higher stiffness (entries 2 *vs.* 3, Table 2). The difference possibly stemmed from the H-bond between furan ring/carbonyls and OH groups, although the π-π aromatic stacking of furan and benzene ring in the linear arrays could not be absolutely denied [32,33].

The mechanical properties of the epoxy resins are shown in Table 2. The tensile strength and hardness of the DGF/DDS outperformed the DGEBA/DDS system. Those performances might be due to the high reactivity of 33DDS and the H-bonds in the DGF/DDS formulations. The increasing amount of rod-like tissues induced by 44DDS easily enhanced the elongation at break. Especially, the DGF/44DDS displayed the highest elongation at break (13.8%). In contrast to DGEBA analogs, the biobased networks from DGF presented hardness as high as 88.3 (HD) (entry 1, Table 2). Those results indicated that the epoxy network rigidity could be enhanced when furan motifs were incorporated.

The investigations of the flammability of the epoxy resins were carried out via microscale combustion calorimetry (MCC). Because it has been proved that the key advancement of MCC is the ability to use substantially less material than other approaches [34]. The curves of

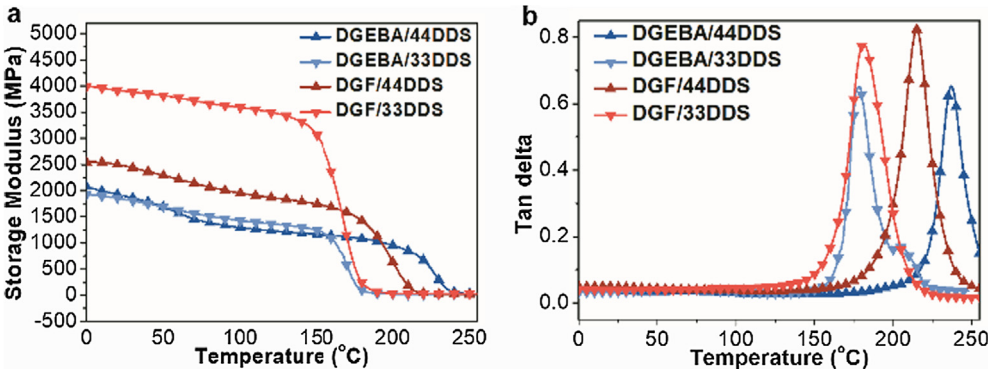

Fig. 4. The curves from DMA experiments. (a) Storage modulus *vs.* temperature with a heating rate of 3. C/min. (b) loss factor (tan δ) *vs.* temperature.

Table 2
Thermomechanical and mechanical properties.

Entry	Sample	T_g[a] (°C)	E'[b] (MPa)	E^{κ}[c] (MPa)	ν_e (mol/dm^3)	Tensile strength (MPa)	Elongation at break (%)	Shore Hardness (HD)
1	DGF/33DDS	180	3921	36	2.48	56	8.5	88.3
2	DGF/44DDS	216	2510	25	1.39	50.2	13.8	86.9
3	DGEBA/33DDS	178	1858	17.56	1.46	49.9	8.2	76.6
4	DGEBA/44DDS	237	1932	16.02	1.18	44.6	10.3	80.5

[a] from DMA.
[b] Values at 20 °C.
[c] Values at T_g + 30 °C.

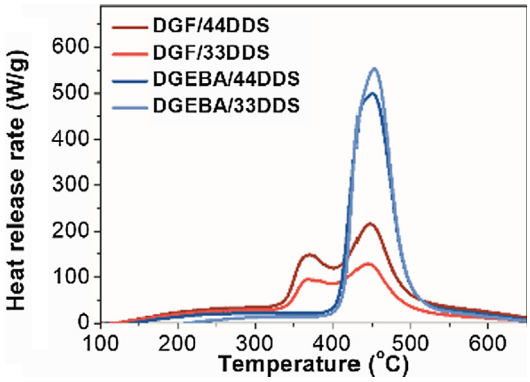

Fig. 5. Heat release rate (HRR) *vs.* temperature curves of epoxy matrixes.

Table 3
Thermal parameters in MCC experiments.

Entry	Samples	HRC (J/g k)	PHRR (W/g)	THR (kJ/g)	Peak temp. (°C)
1	DGF/33DDS	132	128.3	20.5	369/445
2	DGF/44DDS	222	215	31.7	370/445.9
3	DGEBA/33DDS	601	553	32.3	452.8
4	DGEBA/44DDS	516	498.8	36.4	449.3

heat release rate (HRR) *vs.* temperature at a heating rate of 1 °C/s for DGF/DDS and DGEBA/DDS are shown in Fig. 5. The large peaks in the MCC plot have represented that the DGEBA/DDS systems are classified as the most flammable polymers. By contrast, a double peak behavior was observed for the DGF/DDS samples [35,36], which indicated the disparate thermal stabilities of DGF and DDS. The heat release capacities (HRC), average peak heat release rate (PHRR), total heat release (THR) and the peak temperature of heat release for DGF/DDS and DGEBA/DDS are listed in Table 3. Obviously, compared to the HRC, PHRR and THR values of the DGEBA/DDS, DGF/DDS presented milder exothermic processes.

Especially, in contrast to DGEBA/33DDS, the HRC, PHRR and THR values for DGF/33DDS decreased by 78.0%, 76.7% and 36.5%, respectively (entries 1 and 3, Table 3). Most importantly, the descending PHRR value implied a discontinuous flame spread, which hinted the inhibition in the burning process. In addition, for DGF/33DDS, a high residual char about 27% was yielded, which was highly advantageous for flame retardancy (entry 1, Table1). The overall results indicated that the bio-based DGF/DDS presented better flame retardancy than the DGEBA counterpart.

To further investigate the fire retarding mechanism, thermogravimetric analysis coupled to Fourier transform infrared (TGA-IR) was employed to analyze the flammable gas components directly released from the matrixes once the degradation process proceeded [37]. Fig. 6 shows the 3D IR spectra of pyrolysis gases for DGF/33DDS and DGF/44DDS ranging from 40 °C to 800 °C at the heating rate of 10 °C/min. The contrast tests were carried out when the identical size and weight of samples were prepared for the TGA-IR experiments. Thereby, based on the intensity of the character peaks, it is feasible to compare the released gases for accurate determination. As Fig. 6 has shown, the DGF/44DDS delivers much more gases than the relatively intense DGF/33DDS arrays. The DTG results illustrated the separate decomposition processes at T_{max1} (339 °C) and T_{max2} (400 °C), respectively. At the first stage, CO_2 (671, 2303, 2361 cm^{-1}) dominated the pyrolysis gases accompanied by a small number of carbonyl compounds (1734 cm^{-1}) and water (about 3637 cm^{-1}) [38]. The carbonyl peaks corresponded to the thermal cracking of the ester group in DGF segments. As to DGF/44DDS polymers, much more CO_2 was liberated at the first stage (Fig. 6a-ii *vs.* b-ii). The nonflammable CO_2 contributed a lot to a better flame retardancy of DGF/DDS. When the temperature increased to 400 °C, a mixture of combustible components were given off, such as amines (1170 cm^{-1}), alkenes (1328 cm^{-1}, 1377 cm^{-1}), carbonyl compounds (1735–1771 cm^{-1}) and alkynes (2077 cm^{-1}) as well as aromatic alcohols (758, 3580 cm^{-1}). Interestingly, CO_2 was no longer released from the networks. Instead, methane (2969 cm^{-1}), other mixed hydrocarbons (2800–3100 cm^{-1}) and CO (2175 cm^{-1}) started to release in the dissociation. Meanwhile, DDS disintegrated leading to aromatic alcohols and amines. Remarkably, the splitting of the furan core resulted in the formation of alkynes and alkenes. In particular, the characteristic peak for alkynes (2077 cm^{-1}) suggested that DGF/44DDS tended to liberate more alkynes than DGF/33DDS.

3. Conclusions

The bio-based platform FDCA was an eco-friendly alternative feedstock for thermoset synthesis. In contrast to the petro-based DGEBA, the sugar-derivated epoxy monomer DGF endowed the bioepoxy resins with higher thermomechanical properties and flame retardancy as well as better thermal properties. Most importantly, among the reported bioepoxy resins, as yet the DGF/44DDS networks displayed the highest T_g (216 °C), while DGF/33DDS possessed ultra-high stiffness ranging from 0 °C to 180 °C. Those properties ensured the practical DGF/DDS networks applications instead of DGEBA thermosets, and even cutting-edge areas.

4. Data availability

The raw data required to reproduce these findings are available to download from [INSERT PERMANENT WEB LINK(s)]. The processed data required to reproduce these findings are available to download from [INSERT PERMANENT WEB LINK(s)].

Declaration of Competing Interest

The authors declared that there is no Conflict of Interest.

Acknowledgements

This work was supported by the Jiangsu Synergetic Innovation Center for Advanced Bio-Manufacture (grants XTE1827).

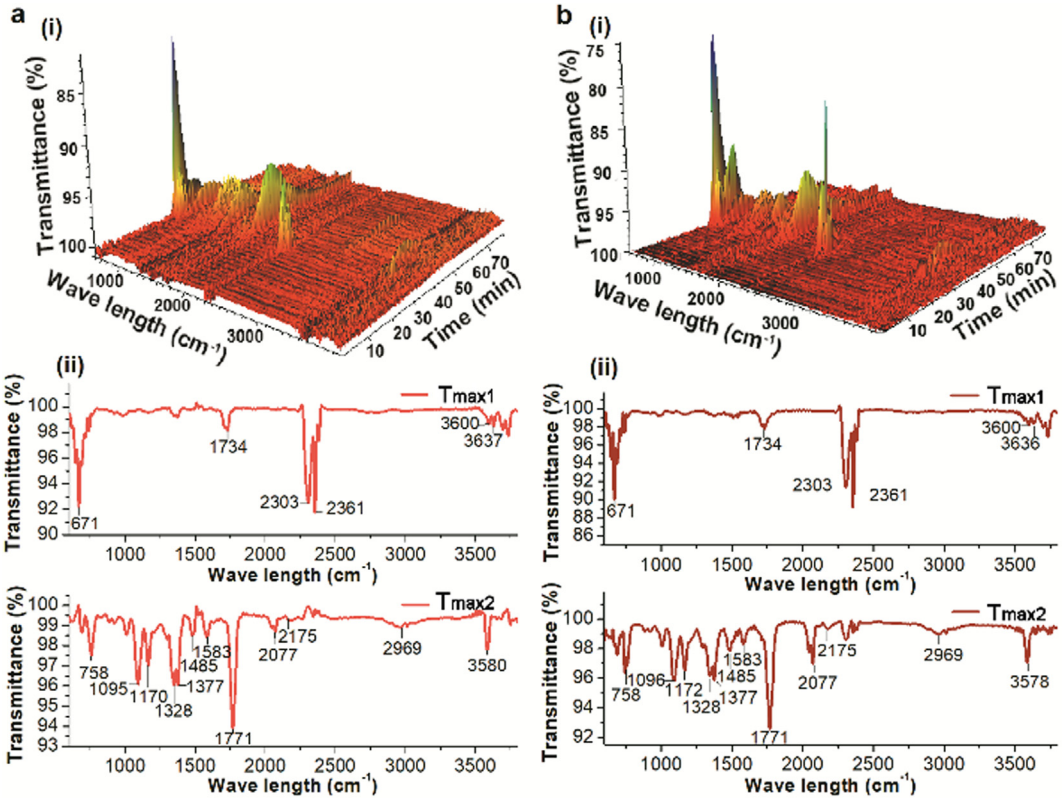

Fig. 6. 3D FT-IR spectra of pyrolysis products of cured DGF/33DDS (a-i) and DGF/44DDS (b-i) resins and the IR spectra at T_{max}s in different stages of DGF/33DDS (a-ii) and DGF/44DDS (b-ii), respectively.

Appendix A. Supplementary material

Supplementary data to this article can be found online at https://doi.org/10.1016/j.eurpolymj.2019.109292.

References

[1] J. Hopewell, R. Dvorak, E. Kosior, Plastics recycling: challenges and opportunities, Philos. Trans. R. Soc. Lond. B Biol. Sci. 364 (2009) 2115–2126.

[2] F. Ng, G. Couture, C. Philippe, B. Boutevin, S. Caillol, Bio-based aromatic epoxy monomers for thermoset materials, Molecules 22 (2017) 149–196.

[3] J. Dai, Y. Peng, N. Teng, Y. Liu, C. Liu, X. Shen, S. Mahmud, J. Zhu, X. Liu, High-performing and fire-resistant biobased epoxy resin from renewable sources, ACS Sustainable Chem. Eng. 6 (2018) 7589–7599.

[4] M.V. Maffini, B.S. Rubin, C. Sonnenschein, A.M. Soto, Endocrine disruptors and reproductive health: the case of bisphenol-A, Mol. Cell. Endocrinol. 254–255 (2006) 179–186.

[5] R. Auvergne, S. Caillol, G. David, B. Boutevin, J. Pascault, Biobased thermosetting epoxy: present and future, Chem. Rev. 114 (2014) 1082–1115.

[6] J. Stanzione III, J. Sadler, J. La Scala, K. Reno, R. Wool, Vanillin-based resin for use in composite applications, Green Chem. 14 (2012) 2346–2352.

[7] M. Fache, A. Viola, R. Auvergne, B. Boutevin, S. Caillol, Biobased epoxy thermosets from vanillin-derived oligomers, Eur. Polym. J. 68 (2015) 526–535.

[8] C. Li, H. Fan, T. Aziz, C. Bittencourt, L. Wu, D.Y. Wang, P. Dubois, Biobased epoxy resin with low electrical permissivity and flame retardancy: from environmental friendly high-throughput synthesis to properties, ACS Sustainable Chem. Eng. 6 (2018) 8856–8867.

[9] J.T. Miao, L. Yuan, G. Liang, A. Gu, Biobased bismaleimide resins with high renewable carbon content, heat resistance and flame retardancy via a multi-functional phosphate from clove oil, Mater. Chem. Front. 3 (2019) 78–85.

[10] S. Ma, X. Liu, L. Fan, Y. Jiang, L. Cao, Z. Tang, J. Zhu, Synthesis and properties of a bio-based epoxy resin with high epoxy value and low viscosity, ChemSusChem 7 (2014) 555–562.

[11] J.M. Sadler, A.T. Nguyen, F.R. Toulan, J.P. Szabo, G.R. Palmese, C. Scheck, S. Lutgen, J.J. La Scala, Isosorbide-methacrylate as a bio-based low viscosity resin for high performance thermosetting applications, J. Mater. Chem. A 1 (2013) 12579–12586.

[12] J. Hong, D. Radojčić, M. Ionescu, Z.S. Petrović, E. Eastwood, Advanced materials from corn: isosorbide-based epoxy resins, Polym. Chem. 5 (2014) 5360–5368.

[13] J. Deng, X. Liu, C. Li, Y. Jiang, J. Zhu, Synthesis and properties of a bio-based epoxy resin from 2,5-furandicarboxylic acid (FDCA), RSC Adv. 5 (2015) 15930–15939.

[14] S. Nameer, D.B. Larsen, J. Duus, A.E. Daugaard, M. Johansson, Biobased cationically polymerizable epoxy thermosets from furan and fatty acid derivatives, ACS Sustainable Chem. Eng. 6 (2018) 9442–9450.

[15] J. Meng, Y. Zeng, G. Zhu, J. Zhang, P. Chen, C. Yao, Z. Fang, K. Guo, Sustainable bio-based furan epoxy resin with flame retardancy, Polym. Chem. 10 (2019) 2370–2375.

[16] F. Hu, J.J. La Scala, J.M. Sadler, G.R. Palmese, Synthesis and characterization of thermosetting furan-based epoxy systems, Macromolecules 47 (2014) 3332–3342.

[17] X. Shen, X. Liu, J. Dai, Y. Liu, Y. Zhang, J. Zhu, How does the hydrogen bonding interaction influence the properties of furan-based epoxy resins, Ind. Eng. Chem. Res. 56 (2017) 10929–10938.

[18] J. Ding, O. Rahman, Q. Wang, W. Peng, H. Yu, Sustainable graphene suspensions: a reactive diluent for epoxy composite valorization, ACS Sustainable Chem. Eng. 5 (2017) 7792–7799.

[19] F.A. Kucherov, L.V. Romashov, K.I. Galkin, V.P. Ananikov, Chemical transformations of biomass-derived C6-furanic platform chemicals for sustainable energy research, materials science, and synthetic building blocks, ACS Sustainable Chem. Eng. 6 (2018) 8064–8092.

[20] J.T. Miao, L. Yuan, Q. Guan, G. Liang, A. Gu, Biobased epoxy resin derived from eugenol with excellent integrated performance and high renewable carbon content, Polym. Int. 67 (2018) 1194–1202.

[21] S. Wang, S. Ma, C. Xu, Y. Liu, J. Dai, Z. Wang, X. Liu, J. Chen, X. Shen, J. Wei, J. Zhu, Vanillin-derived high-performance flame retardant epoxy resins: facile synthesis and properties, Macromolecules 50 (2017) 1892–1901.

[22] J. Wan, J. Zhao, B. Gan, C. Li, J. Molina-Aldareguia, Y. Zhao, Y.T. Pan, D.Y. Wang, Ultrastiff biobased epoxy resin with high T_g and low permittivity: from synthesis to properties, ACS Sustainable Chem. Eng. 4 (2016) 2869–2880.

[23] J.T. Miao, L. Yuan, Q. Guan, G. Liang, A. Gu, Biobased heat resistant epoxy resin with extremely high biomass content from 2,5-furandicarboxylic acid and eugenol, ACS Sustainable Chem. Eng. 5 (2017) 7003–7011.

[24] M.K. Hassan, S.J. Tucker, A. Abukmail, J.S. Wiggins, K.A. Mauritz, Polymer chain dynamics in epoxy based composites as investigated by broadband dielectric spectroscopy, Arab. J. Chem. 9 (2016) 305–315.

[25] Y. Yanagisawa, Y. Nan, K. Okuro, T. Aida, Mechanically robust, readily repairable polymers via tailored noncovalent cross-linking, Science 359 (2018) 72–76.

[26] P. Sharma, V. Choudhary, A.K. Narula, Curing of epoxy resin using imide-amines, J. Appl. Polym. Sci. 101 (2006) 3503–3510.

[27] (a) S. Zhao, X. Huang, A.J. Whelton, M.M. Abu-Omar, Renewable Epoxy Thermosets from Fully Lignin-Derived Triphenols, ACS Sustainable Chem. Eng. 6 (2018) 7600–7608 In contrast, DGF has advantagous stiffness than the recently reported renewable lignin- and daidzein-derivated epoxy thermosets, seeing:; (b) K.H. Nicastro, C.J. Kloxin, T.H. Epps, Potential lignin-derived alternatives to bisphenol A in diamine-hardened epoxy resins, ACS Sustainable Chem. Eng. 6 (2018) 14812–14819;

(c) Ref. 3.
[28] Comparing with the E' of diglycidyl ether of daidzein (DGED)/DDM, the epoxy resin herein are more excellent not only for higher E' values, but also for the long working temperatures, seeing Ref. 3.
[29] X. Yu, S. Sreenivasan, K. Tian, T. Zheng, J.G. Lawrence, S. Pilla, Sustainable animal protein-intermeshed epoxy hybrid polymers: from conquering challenges to engineering properties, ACS Omega 3 (2018) 14361–14370.
[30] A.L. Cholli, J.J. Dumais, A.K. Engel, L.W. Jelinski, Aromatic ring flips in a semicrystalline polymer, Macromolecules 17 (1984) 2399–2404.
[31] E.D. Hernandez, A.W. Bassett, J.M. Sadler, J.J. La Scala, J.F. Stanzione, Synthesis and characterization of bio-based epoxy resins derived from vanillyl alcohol, ACS Sustainable Chem. Eng. 4 (2016) 4328–4339.
[32] A.S. Shetty, J. Zhang, J.S. Moore, Aromatic π-stacking in solution as revealed through the aggregation of phenylacetylene macrocycles, J. Am. Chem. Soc. 118 (1996) 1019–1027.
[33] Z.F. Yao, J.Y. Wang, J. Pei, Control of π–π stacking via crystal engineering in organic conjugated small molecule crystals, Cryst. Growth. Des. 18 (2018) 7–15.
[34] R.H. Krämer, M. Zammarano, G.T. Linteris, U.W. Gedde, J.W. Gilman, Heat release and structural collapse of flexible polyurethane foam, Polym. Degrad. Stabil. 95 (2010) 1115–1122.
[35] J.H. Cho, V. Vasagar, K. Shanmuganathan, A.R. Jones, S. Nazarenko, C.J. Ellison, Bioinspired catecholic flame retardant nanocoating for flexible polyurethane foams, Chem. Mater. 27 (2015) 6784–6790.
[36] B. Schartel, T.R. Hull, Development of fire-retarded materials-Interpretation of cone calorimeter data, Fire Mater. 31 (2007) 327–354.
[37] C.A. Wilkie, TGA/FTIR: an extremely useful technique for studying polymer degradation, Polym. Degrad. Stabil. 66 (1999) 301–306.
[38] D. Rosu, F. Mustata, N. Tudorachi, V.E. Musteata, L. Rosu, C.D. Varganici, Novel bio-based flexible epoxy resin from diglycidyl ether of bisphenol A cured with castor oil maleate, RSC Adv. 5 (2015) 45679–45687.